

## J1.4 ANALYSIS OF LIGHTNING CLOUD-TO-GROUND FLASH ACTIVITY FOR NATIONAL AVIATION CHOKE POINT REGION STUDIES

Thomas A. Seliga<sup>1\*</sup>, David A. Hazen<sup>2</sup> and Cynthia Schauland<sup>3</sup>

1. Volpe National Transportation Systems Center, Cambridge, MA
2. Titan/System Resources Corporation, Billerica, MA
3. Federal Aviation Administration, Washington, DC

### 1. INTRODUCTION

This paper demonstrates the potential utility of employing lightning flash spatial and temporal density variations for evaluating the effects of thunderstorms on air traffic operations, particularly as they relate to the National Choke Point regions of the contiguous United States (CONUS). The major region of interest covers the area extending from east of Boston, MA and then west to just beyond Minneapolis-St. Paul (MSP), covering longitudes from 60-100° W. The north-south latitudinal extent ranges from central Georgia to northern Michigan (about 34-46°N). This region encompasses the highest volume of air traffic within the CONUS and is subject to higher delays due to severe weather than any other region.

The lightning data used here were obtained from archived reports on lightning cloud-to-ground flashes reported by Global Atmospheric, Inc. (GAI) through its National Lightning Detection Network (NLDN). The NLDN detects and reports the occurrence of cloud-to-ground lightning flashes throughout the CONUS (Orville, 1991; Orville and Silver, 1997; Orville and Huffines, 1999; Orville and Huffines, 2001). The lightning data are represented on distance vs time plots or Hovmöller diagrams, similar to those used in a previous study (Seliga et al., 2002). In this paper, the focus is on the latitudes and longitudes that cover the National Choke Point Region described above. The Hovmöller plots have a spatial resolution of 0.05° in both latitude and longitude and temporal resolution of 15 minutes. Flash density plots within the region of interest over periods of 15, 30 and 60-minutes also provide essential information on the actual location and movement of thunderstorms.

### 2. LIGHTNING DATA

The U.S. DOT Volpe Center has utilized and analyzed NLDN data for over 10 years, primarily in support of the FAA's program to automate the detection and reporting of thunderstorms through Automated Weather Observing Systems (AWOS) and Automated Surface Observing Systems (ASOS) (Canniff, 1993; Kraus and Canniff, 1995; Kraus et al., 2000; Seliga et al., 2000). Essentially, NLDN data signify the occurrence of cloud-to-ground lightning flashes and represent the occurrence of thunderstorms throughout the U.S. The data have proven useful for numerous applications (e.g.,

Changnon, 1988a, b; Holle and Lopez, 1993; Orville, 1997; Orville et al., 1999; Rhoda and Pawlak, 1999; Seliga and Shorter, 2000; Orville and Huffines, 2001; Bates et al., 2001).

The NLDN flash data used here were for 5-9 July 1999.

### 3. METHODOLOGY

The lightning data were examined using time-distance or Hovmöller diagrams, similar to those generated by Carbone et al. (2001a) in analyzing NEXRAD data for warm season storm characterizations over a large portion of the CONUS. Seliga et al. (2002) demonstrated strong correlations between lightning and NEXRAD data with this technique. The applicable time scales can range from hours to a few days to a few months. The diagrams have been found useful for climatological studies that examine one or more variables such as rainfall, temperature and winds. The Hovmöller diagram produced from NLDN data for the period 5-9 July 1999, covering the latitude range from 34-46° N and longitudes from 60-100° W, is shown in Fig. 1.

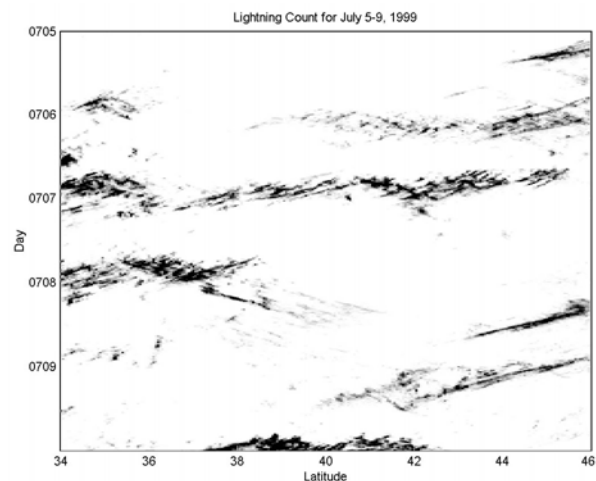


**Fig. 1** – Cloud-to-ground lightning flash Hovmöller diagram covering the National Choke Point Region (34:46° N, 60-100° W).

A thorough interpretation of the data in Fig. 1 requires additional insights that are not dealt with here. Other examples of possibly relevant data include the corresponding Hovmöller diagram vs longitude (Fig. 2),

\* Corresponding Author Address: Thomas A. Seliga, Surveillance and Sensors Division, DTS-53, Volpe National Transportation Systems Center, 55 Broadway, Cambridge, MA 02142-1093; **Email:** seliga@volpe.dot.gov

mappings of the spatial distribution of the data at different time intervals, satellite and radar data, other meteorological parameters within or affecting the same spatial and temporal domains, topographical features and representations of weather from applicable numerical models. Nevertheless, the data in Fig. 1 by itself reveals a number of important features. A distinct diurnal pattern is evident in the lightning events with events repeating themselves daily, centered around ~ 1800-2200 GMT, extending between ~ 34-36° N and ~ 35-46° N on 5-6 Jul and extending nearly over all the latitudes on 6-7 Jul from 34-39° N on 7-8 Jul and 34-36° N on 8 Jul.

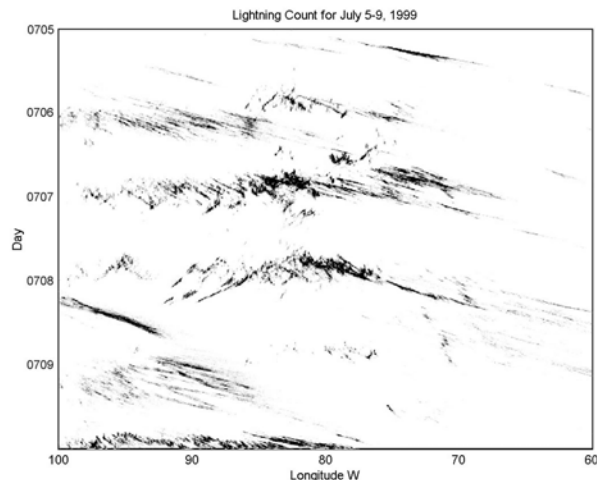


**Fig. 2** – Sample Hovmöller longitude diagram of choke point region

Another generic set of features in Fig. 1 is the evidence of storm motion, ranging from stationarity to cell movements of various speeds in both S to N and N to S directions. The speeds of the motion are readily determined from the slopes of the streaks or through 2-D autocorrelations of the diagrams; these speeds vary considerably while also at times exhibiting strong coherency from day to day, from storm cell to storm cell or within a given system. Special events are also immediately evident. One such event is that travel from S to N or from S to N in different latitude bands. Interpretation and understanding of such features require careful examination of both Hovmöller diagrams and the associated spatial description of the relevant storms.

Intensity is also of fundamental interest. The intensity in Figs. 1-2 represents the number of flashes occurring in 0.05° latitudinal and longitudinal swaths over 15 min time intervals. If, as expected, lightning activity were to be a measure of convective strength in warm season events, then the intensity variation would represent the relative intensity of convection. For example, Fig. 1 shows a diurnal variability in storm occurrences beginning with high latitude activity on the 5<sup>th</sup> and then spreading out dramatically in latitude on the 6<sup>th</sup>. Meanwhile, a second area of activity appeared over lower latitudes. On the 7<sup>th</sup>, the activity in the lower and

higher latitudes nearly converged. The higher latitude activity decayed on the 8<sup>th</sup> while the lower latitude area expanded north and intensified. Later that same day, another line of activity formed in the upper latitudes and recurred at about ½ day intervals in a southward direction.

Fig. 2 shows the corresponding longitudinal Hovmöller diagram for the same time period. To account for differences between latitude and longitude widths, the lightning flash counts were normalized using a scale factor of 2.55. The diurnal pattern is evident over a wide longitude range from 5-9 Jul. The west-east speed of the thunderstorm cells and systems are simply derived from the slopes of individual cells. The diurnal activity was most intense in the middle longitude area on the 6<sup>th</sup> and 7<sup>th</sup>. Although the diurnal pattern is evident throughout the entire period, its longitudinal extent reduced considerably on the 8<sup>th</sup>. The motion is predominantly west to east, although there are occasions where east to west motions also occur. There is an isolated area of coherent activity at about 0400 GMT on the 8<sup>th</sup> continuing from 100° W and holding together until about 1400 GMT the same day and decaying rapidly at about 92° W. Overall, the activity is weak east of about 68° W. It is worth noting that structural decay of individual cells as seen from measures of storm breadth normal to the direction of travel is more evident in Fig. 1 than Fig. 2, indicating that latitudinal plots may provide important hints regarding storm cell evolution compared to longitudinal plots. Another feature evident in this data set is that storms located towards the south tend to move slower than those located farther north.

#### 4. SELECTED CASES

Latitude-longitude plots of 15-, 30- and 60-minute flash counts were examined during the 5-9 Jul 1999 period to locate and identify storms. The plots were then animated to explore the behavior of these events. Major cities within this National Choke Point region are also identified. Sample plots are shown in Figs. 3a-c. The following sample storms illustrate how insights into storm behavior can be gleaned from the lightning data presented in the ways indicated. The discussion is limited, since the purpose is to illustrate potential rather than perform in-depth analyses. The latter are outside the scope of the current effort.

##### 4.1 – Storm Behavior

A rather intense storm affected Montreal on the 5<sup>th</sup> at about 0630 GMT. This storm is located in the upper right-hand part of Fig. 1 and just to the right of the center of Fig. 2. Fig. 1 shows considerable breadth as well as transit from north to south while Fig. 2 shows that this same storm was narrow in longitudinal extent and traveled much faster from west to east than from north to south. Although not shown here, measurements of the storm's progress over time provides valuable nowcasting insights (storm presence, location, direction and speed of travel, relative intensity) into its future behavior. It appears that the nowcasting ability is

dependent on both the storm's history and its stage of development. Time horizons of 1-4 or more hours appear realistic.

On this same day, 5 Jul, a less intense storm grazed MSP at about 1130 GMT. This storm is the light gray regions just below the Montreal event in Fig. 1 and the isolated region in Fig. 2 that begins at around 94° W. Fig. 1 shows that this storm grew in latitudinal extent as it moved northward. Fig. 2 shows that its longitudinal extent remained small throughout its evolution while at the same time the storm exhibited strong westerly motion.

During the period covered in Figs. 1-2, the greatest impact on the National Choke Point region occurred during the passage of the gust front, line of thunderstorms that is shown in Fig. 3. The first portion of this event is shown at the base of Figs. 1-2. Although not easily evident in the figures, there are very distinct features in both of these Hovmöller plots that signify individual thunderstorm cells, including information on their properties and evolution. The cells remain coherent over hours and travel in easily recognized fashion. Diurnal behavior is predictable and provides guidance on when onset begins, maximum intensity is reached, decay begins and storms terminate.

Since there is a very high correlation between lightning activity and NEXRAD reflectivity data in warm season precipitation events (Seliga et al, 2002), except for a lack of direct information on the height of storms, such lightning data provides important tactical information for the guidance of air traffic during times when critical airspace is affected by the passage of thunderstorms. The relevancy of this insight would be most useful when radar data are unavailable because of the absence of radar measurements due to coverage, failure or maintenance. If in the future, in-cloud lightning data are available, significant improvements in estimating the height of storms would also be available to further improve the value of lightning data for air traffic operational applications. In-cloud lightning data would also provide important earlier detection of storm development as well as higher lightning density plots for contouring lightning activity.

#### 4.2 – Time Sensitivity

Figs. 3 a-c are a series of lat-long plots of flash counts from 2345-2400 GMT on 9 Jul 1999, from 2330-2400 GMT and from 1800-2400 GMT. Fig 3 c covered a storm from start through the end of the day. These plots represent thunderstorm tracks over different durations of time and illustrate a simple, static means for displaying impacted areas as well as for comparing the most recent samples with averaged/integrated spatial samples that extend backwards in time. Similar plots that cover the entire storm or storm system are used to display rainfall accumulations. As seen in Fig. 3 c, these integrated pictures of lightning activity are useful for identifying embedded distinct thunderstorm cells, gauging storm diffusivity and tracking storm motion geographically. They are considered important

supplements to the Hovmöller diagrams presented previously.

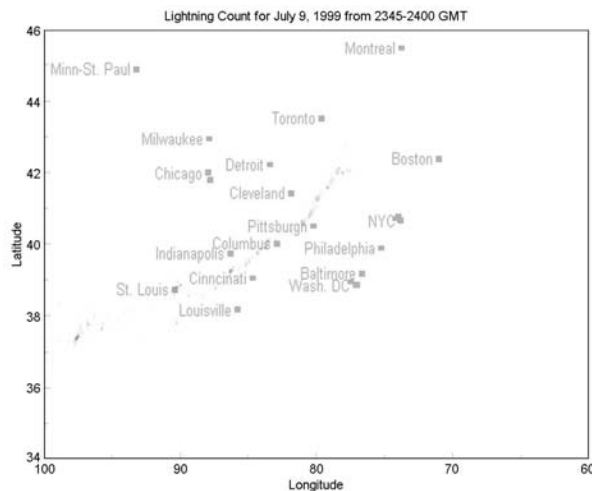


Fig. 3a – Sample Latitude-Longitude plot, 15 min counts

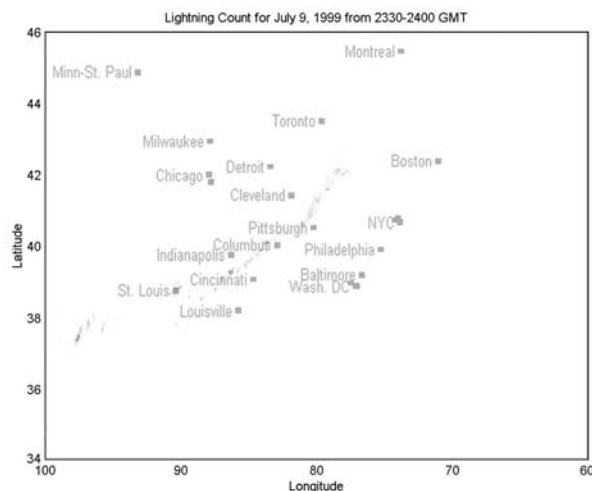


Fig. 3b – Sample Latitude-Longitude plot, 30 min counts

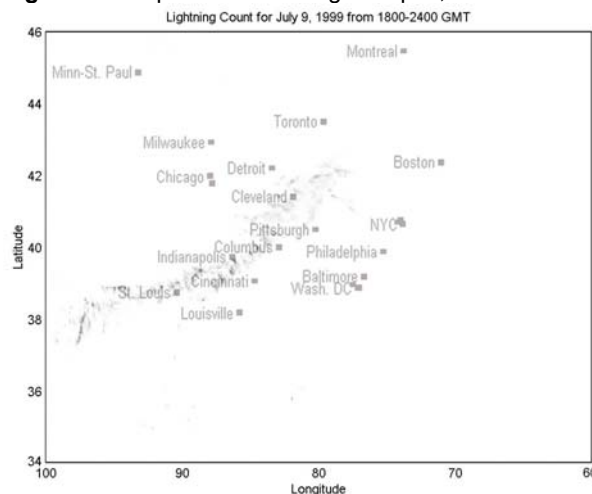


Fig. 3c – Sample Latitude-Longitude plot, storm

## 5. SUMMARY

This study examined lightning activity within the National Choke Point region encompassing the eastern part of CONUS in order to demonstrate how time-distance or Hovmöller plots with latitude and longitude can be used with other representations of lightning data to provide both past and real-time observations of thunderstorm activity. It appears that such data has relevance for improving nowcasting of thunderstorms out to several hours; this is based on both the general features of storm behavior evident in the plots and a cursory examination of several storm events. Hovmöller plots with time resolution of 15 minutes and spatial resolution of  $0.05^\circ$  in latitude and longitude can show the onset, decay and temporal evolution of thunderstorms over periods of hours, days, months and seasons. The speeds and intensity of thunderstorm cells and systems are also easily deduced from these plots. Since aviation is often highly affected by thunderstorms, the approach illustrated here with lightning data suggests that significant improvements in aviation operational practices should result from insights and procedures gleaned from studies that include this approach in their analyses and derivation of operational weather products. Clearly, the use of lightning data alone for such applications is insufficient. The effective integration of the lightning data with other meteorological data is essential, although not included herein.

## 6. REFERENCES

- Bates, E. G., T. A. Seliga and T. Weyrauch, 2001: Implementation of grounding, bonding, shielding and power system improvements in FAA systems: Reliability assessments of the Terminal Doppler Weather Radar (TDWR). 20<sup>th</sup> Digital Avionics Systems Conference, Daytona Beach, FL, 14-18 October.
- Canniff, J. F., 1993: Thunderstorm detection: FAA applications for network lightning data. Preprints 8<sup>th</sup> Symposium on Meteorological Observations and Instrumentation, AMS Annual Mtg., Anaheim, CA, 91-92.
- Carbone, R. E., J. D. Tuttle, D. A. Ahijevych and S. B. Trier, 2001a: Inferences of predictability associated with warm season precipitation episodes, in press *J. Atmos. Sci.*, 2002.
- Carbone, R. E., J. D. Tuttle, D. A. Ahijevych and S. B. Trier, 2001b: Website for charts and base data; <http://www.mmm.ucar.edu/episodes/index.html>.
- Changnon, S. A., 1988a: Climatography of thunder events in the conterminous United States. Part I: Temporal aspects. *J. Climate*, **1**, 389-398.
- Changnon, S. A., 1988b: Climatography of thunder events in the conterminous United States. Part II: Spatial aspects. *J. Climate*, **1**, 399-405.
- Holle, R. L. and R. E. Lopez, 1993: Overview of real-time lightning detection systems and their meteorological uses. NOAA Tech. Memo. ERL NSSL-102, 68 pp.
- Houze, R. A., Jr., 1993: *Cloud Dynamics*, Acad. Press, Inc., 573 pp.
- Kraus, K. and J. Canniff, 1995: Incorporating lightning data into automated weather observations. Preprints 6<sup>th</sup> Conference on Aviation Weather Systems, AMS, 466-469.
- Kraus, K., T. A. Seliga and J. R. Kranz, 2000: Final performance evaluation of the Automated Lightning Detection and Reporting System (ALDARS). Preprints 16<sup>th</sup> International Conference on Interactive Information and Processing Systems (IIPS) for Meteorology, Oceanography, and Hydrology, Long Beach, CA, AMS Annual Mtg., 106-109.
- Orville, R. E., 1991: Lightning ground flash density in the contiguous United States – 1989. *Mon. Wea. Rev.*, **119**, 573-577.
- Orville, R. E. and A. C. Silver, 1997: Lightning ground flash density in the contiguous United States – 1992-95. *Mon. Wea. Rev.*, **125**, 631-638.
- Orville, R. E. and G. R. Huffines, 1999: Lightning ground flash measurements over the contiguous United States: 1995-97. *Mon. Wea. Rev.*, **127**, 2693-2703.
- Orville, R. E. and G. R. Huffines, 2001: Cloud-to-ground lightning in the United States: NLDN results in the first decade, 1989-98. *Mon. Wea. Rev.*, **129**, 1179-1193.
- Rhoda, D. A. and M. L. Pawlak, 1999: An assessment of thunderstorm penetrations and deviations by commercial aircraft in the terminal area. MIT Lincoln Laboratory Project Rept., NASA/A-2, 98 pp.
- Seliga, T. A. and J. A. Shorter, 2000: Contribution to a baseline understanding of the impact of weather on airline carrier operations, Preprints 2<sup>nd</sup> Symposium on Environmental Applications, AMS Annual Mtg., 9-14 January 2000, Long Beach, CA, 190-193.
- Seliga, T. A., D. A. Hazen, and C. Schauland., 2002, "Comparisons of Cloud-to-Ground Lightning Flash Data With NEXRAD Inferences on Rainfall as Functions of Longitude and Latitude". Preprints 6<sup>th</sup> Symposium on Integrated Observing Systems, American Meteorological Society, Orlando, FL 13-17 January 2002.
- Solomon, R. and M. Baker, 1998: Lightning flash rate and type in convective storms. *J. Geophys. Res.*, **103**, 14,041-14,057.